

# Mechanism-based sirtuin enzyme activation

Raj Chakrabarti\*

Division of Fundamental ResearchPMC Advanced Technology, LLC. 1288 Route 73 South, Mt. Laurel, NJ 08054, USA Phone: (609) 216-4644 Email: raj@pmc-group.com

Submitted to Proceedings of the National Academy of Sciences of the United States of America

**Sirtuin enzymes are NAD<sup>+</sup>-dependent protein deacylases that play a central role in the regulation of healthspan and lifespan in organisms ranging from yeast to mammals. There is intense interest in the activation of the seven mammalian sirtuins (SIRT1-7) in order to extend mammalian healthspan and lifespan. However, there is currently no understanding of how to design sirtuin-activating compounds beyond allosteric activators of SIRT1-catalyzed reactions that are limited to particular substrates. Moreover, across all families of enzymes, only a dozen or so distinct classes of non-natural small molecule activators have been characterized, with only four known modes of activation among them. None of these modes of activation are based on the unique catalytic reaction mechanisms of the target enzymes. Here, we report a general mode of sirtuin activation that is distinct from any of the known modes of enzyme activation. Based on the conserved mechanism of sirtuin-catalyzed deacylation reactions, we establish biophysical properties of small molecule modulators that can result in enzyme activation for any sirtuin and any substrate. Building upon this framework, we propose mechanism-based workflows for the design of new sirtuin-activating compounds.**

Sirtuins | Sirtuin activators | Kinetic modelling

## Introduction

Sirtuin (silent information regulator) enzymes, which catalyze NAD<sup>+</sup>-dependent protein post-translational modifications, have emerged as critical regulators of many cellular pathways. In particular, these enzymes protect against age-related diseases and serve as key mediators of longevity in evolutionarily distant organismic models [1]. Sirtuins are NAD<sup>+</sup>-dependent lysine deacylases, requiring the cofactor NAD<sup>+</sup> to cleave acyl groups from lysine side chains of their substrate proteins, and producing nicotinamide (NAM) as a by-product. A thorough understanding of sirtuin chemistry is not only of fundamental importance, but also of considerable medicinal importance, since there is enormous current interest in the development of new mechanism-based sirtuin modulators [2, 3]. The mechanism of sirtuin-catalyzed, NAD<sup>+</sup>-dependent protein deacylation is depicted in Fig. 1 [4-6].

Recently, in order to extend mammalian healthspan and lifespan, intense interest has developed in the activation of the seven mammalian sirtuin enzymes (SIRT1-7) [7,8,9]. Prior work on sirtuin activation has relied exclusively on experimental screening, with an emphasis on allosteric activation of the SIRT1 enzyme. Indeed, small molecule allosteric activators of SIRT1 have been demonstrated to induce lifespan extension in model organisms such as mice [7, 8]. Allosteric activation is one of four known modes by which small molecules can activate enzymes [10]. Allosteric activators most commonly function by decreasing the dissociation constant for the substrate (the acylated protein dissociation constant  $K_{d,Ac-B}$  in the case of sirtuins).

Nearly all known sirtuin activators allosterically target SIRT1 and bind outside of the active site to an allosteric domain in SIRT1 that is not shared by SIRT2-7 [9]. Moreover, allosteric activators only work with a limited set of SIRT1 substrates [11-13]. It is now known that other sirtuins -- including SIRT2, SIRT3 and SIRT6 -- and multiple protein substrates play significant roles in regulating mammalian longevity [14-16]. General strategies for the activation of any mammalian sirtuin (including activation of

SIRT1 for other substrates) are hence of central importance, but not understood [17]. In general, allosteric activation to decrease substrate  $K_d$  will not be an option for enzyme activation, rendering mechanism-based activation essential.

Foundations for the rational design of mechanism-based sirtuin activators have been lacking, partly due to the absence of a clear understanding of the kinetics of sirtuin-catalyzed deacylation. Several types of mechanism-based sirtuin inhibitors have been reported recently in the literature, including Ex-527 and Sir-Real2 [18, 19]. However, mechanism-based activation has proven far more elusive, due to the difficulty in screening for the balance of properties needed for a modulator to have the net effect of accelerating catalytic turnover. While there are many ways to inhibit an enzyme's mechanism, there are far fewer ways to activate it. These efforts have been hindered by the lack of a complete steady state kinetic model of sirtuin catalysis that accounts for the effects of both NAD<sup>+</sup> and NAM on activity.

In the so-called "NAD<sup>+</sup> world" picture of global metabolic regulation, the intracellular concentrations of the sirtuin cofactor NAD<sup>+</sup>, which can decrease with age, play a central role in regulating mammalian metabolism and health through sirtuin-dependent pathways [20]. Due to the comparatively high Michaelis constants for NAD<sup>+</sup> ( $K_{m,NAD^+}$ 's) of mammalian sirtuins, their activities are sensitive to intracellular NAD<sup>+</sup> levels [4, 20]. The systemic decrease in NAD<sup>+</sup> levels that accompanies organismic aging downregulates sirtuin activity and has been identified as a central factor leading to various types of age-related health decline [21, 22, 23], whereas increases in NAD<sup>+</sup> levels can upregulate sirtuin activity and as a result mitigate or even reverse several aspects of this decline [20, 24].

As such, NAD<sup>+</sup> supplementation has emerged as a promising alternative to allosteric activation of sirtuins [24]. Unlike

## Significance

**Compared to enzyme inhibitors, which constitute the vast majority of today's drugs, enzyme activators have considerable advantages. However, they are much more difficult to design, because enzymatic catalysis has been optimized over billions of years of evolution. Sirtuin-activating compounds (STACs) are enzyme activators that can extend mammalian healthspan and lifespan. Unfortunately, the only known mode of STAC action is limited to accelerating selected functions of a single mammalian sirtuin enzyme. Here, we report a wholly new mode of enzyme activation that exploits the common catalytic mechanism of all sirtuin enzymes, hence being applicable to any function of any sirtuin. This expands our understanding of enzyme activation, and lays the foundation for development of a new generation of drugs.**

## Reserved for Publication Footnotes

137  
138  
139  
140  
141  
142  
143  
144  
145  
146  
147  
148  
149  
150  
151  
152  
153  
154  
155  
156  
157  
158  
159  
160  
161  
162  
163  
164  
165  
166  
167  
168  
169  
170  
171  
172  
173  
174  
175  
176  
177  
178  
179  
180  
181  
182  
183  
184  
185  
186  
187  
188  
189  
190  
191  
192  
193  
194  
195  
196  
197  
198  
199  
200  
201  
202  
203  
204

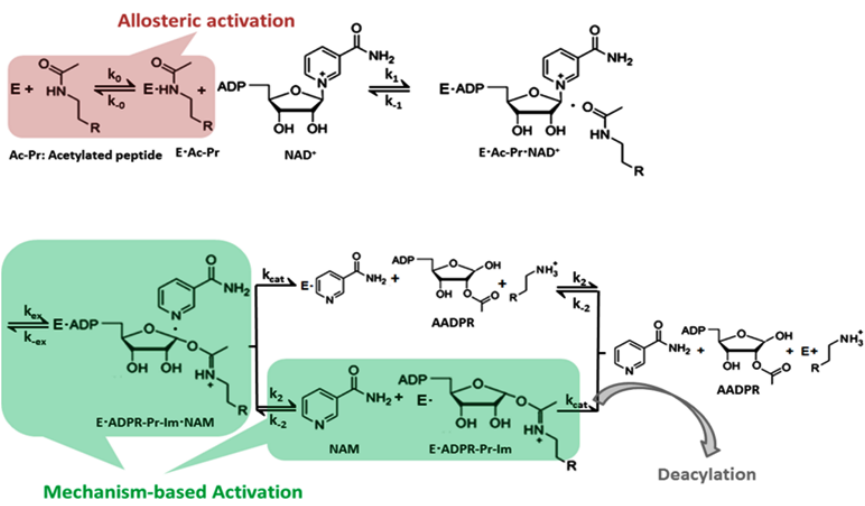


**Fig. 1.** Chemical mechanism of sirtuin-catalyzed deacylation and modes of sirtuin activation. Following sequential binding of acylated peptide substrate and NAD<sup>+</sup> cofactor, the reaction proceeds in two consecutive stages: i) cleavage of the nicotinamide moiety of NAD<sup>+</sup> (ADP-ribosyl transfer) through the nucleophilic attack of the acetyl-Lys side chain of the protein substrate to form a positively charged O-alkylimidate intermediate (depicted above), and ii) subsequent formation of deacylated peptide. For simplicity, all steps of stage ii as well as AADPR + Pr dissociation are depicted to occur together with rate limiting constant  $k_{cat}$ . **Red:** Allosteric activation increases the affinity of a limited set of peptide substrates for the SIRT1 enzyme only and requires an allosteric binding site. **Green:** Mechanism-based activation is a new mode of enzyme activation that relies on the conserved sirtuin reaction mechanism rather than an increase in the affinity of selected peptide substrates.

205  
206  
207  
208  
209  
210  
211  
212  
213  
214  
215  
216  
217  
218  
219  
220  
221  
222  
223  
224  
225  
226  
227  
228  
229  
230  
231  
232  
233  
234  
235  
236  
237  
238  
239  
240  
241  
242  
243  
244  
245  
246  
247  
248  
249  
250  
251  
252  
253  
254  
255  
256  
257  
258  
259  
260  
261  
262  
263  
264  
265  
266  
267  
268  
269  
270  
271  
272

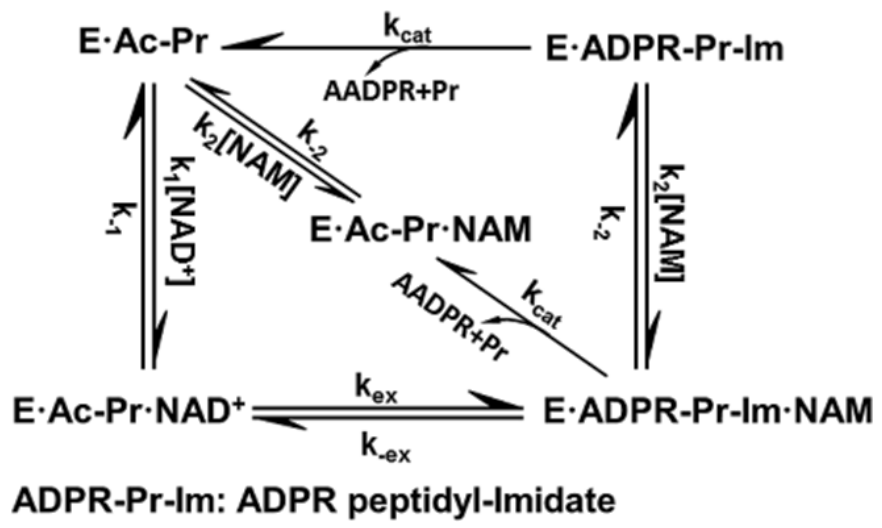


**Fig. 2.** General model for sirtuin-catalyzed deacylation in the presence of NAD<sup>+</sup> and NAM. This model, based on the reaction mechanism depicted in Fig. 1, provides a minimal kinetic model that captures the essential features of sirtuin deacylation kinetics suitable for predicting the effects of mechanism-based modulators on sirtuin activity. In the presence of saturating Ac-Pr, E is rapidly converted into E·Ac-Pr and NAM binding to E can be neglected, resulting in a simplified reaction network with 5 species. Ac-Pr, acetylated peptide; ADPR, adenosine diphosphate ribose; AADPR, O-acetyl adenosine diphosphate ribose.

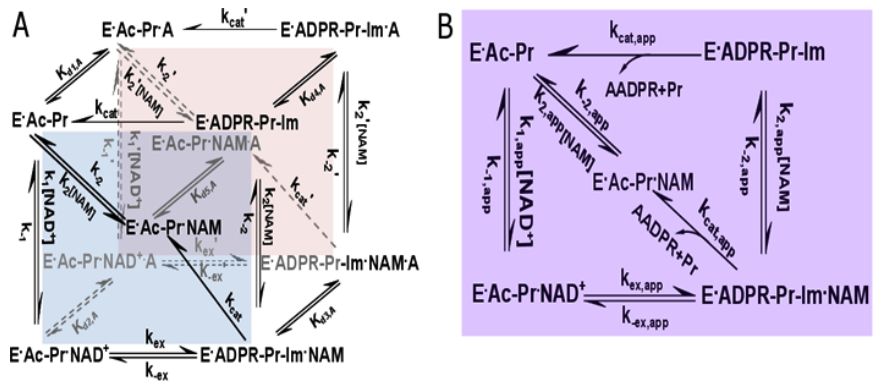


**Fig. 3.** General model for mechanism-based sirtuin enzyme activation. A) The front face of the cube (blue) depicts the salient steps of the sirtuin reaction network in the absence of bound modulator. The back face of the cube (red) depicts the reaction network in the presence of bound modulator (denoted by "A"). Each rate constant depicted on the front face has an associated modulated value on the back face, designated with a prime that is a consequence of modulator binding. B) The purple face is the apparent reaction network in the presence of a nonsaturating concentration of modulator.

allosteric activators like resveratrol, which are SIRT1-specific and have not been successfully applied to other sirtuins [10],

NAD<sup>+</sup> supplementation can activate most mammalian sirtuins in a substrate-independent fashion. Moreover, allosteric activa-

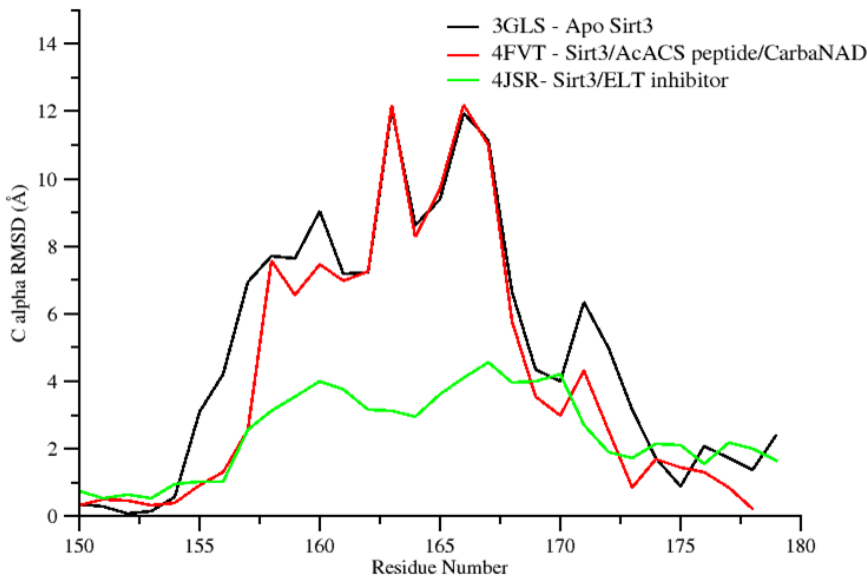


**Fig. 4.** Sirt3 cofactor binding loop region RMSD. Sirt3 proteins and their per-residue RMSD values for the cofactor binding loop region computed over all atoms with reference to crystal structure of a Sirt3 intermediate complex (4BVG). Residues (155-178) correspond to the co-factor binding loop region and residues (162-170) form a short alpha helix when bound to cofactors.

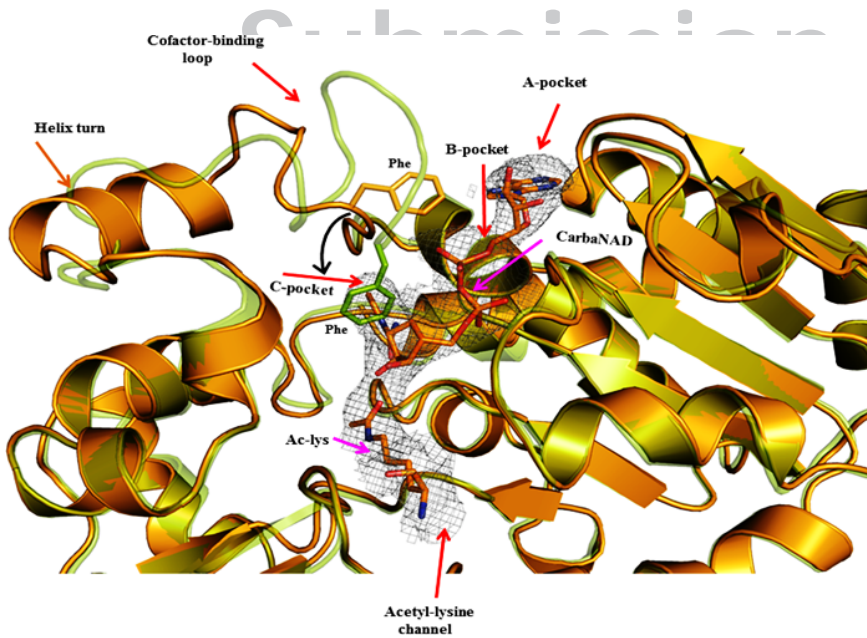


**Fig. 5.** : Structural superposition of Sirt3 structures. Superposition of Sirt3 native intermediate (4BVG - Green) and Sirt3 ternary complex (4FVT - Orange) showing differences in the conformation of the cofactor binding loop and the position of the Phe residue. Individual subsites are highlighted and the movement of Phe residue is indicated by black arrows. The substrates Carba-NAD and Ac-Lysine are rendered in stick representation.

tors cannot fully compensate for the reduction in sirtuin activity that occurs through  $\text{NAD}^+$  decline during aging. On the other hand, the effects of  $\text{NAD}^+$  supplementation are not specific to sirtuins and prohibitively high concentrations of  $\text{NAD}^+$ , along with associated undesirable side effects, may be required to elicit the increases in sirtuin activity required to combat age-related diseases.

A preferred general strategy for activation of sirtuins (Fig. 1) would be to increase their sensitivity to  $\text{NAD}^+$  through a reduction of  $K_{m,\text{NAD}^+}$ .  $K_{m,\text{NAD}^+}$  reduction would have a similar activating effect to  $\text{NAD}^+$  supplementation, but would be selective for sirtuins and could potentially even provide isoform specific sirtuin activation. Importantly, due to the sirtuin nicotinamide cleavage reaction that involves the  $\text{NAD}^+$  cofactor, modulation of  $K_{m,\text{NAD}^+}$  may in principle be achievable by means other than altering the binding affinity of  $\text{NAD}^+$ . Unlike allosteric activation that reduces  $K_{d,\text{Ac-Pe}}$ , this approach would be applicable to any sirtuin and any substrate.

In this paper, we present a general framework for activation of sirtuin enzymes that is distinct from any of the known modes of enzyme activation, based on the fundamental mechanism of the sirtuin deacylation reaction. We first introduce a steady-state model of sirtuin-catalyzed deacylation reactions in the presence of  $\text{NAD}^+$  cofactor and endogenous inhibitor NAM, and then establish quantitatively how  $K_{m,\text{NAD}^+}$  can be modified by small molecules, identifying the biophysical properties that small molecules must have to function as such mechanism-based activators. We propose workflows suitable for mechanism-based design of sirtuin activating compounds and present computational evidence supporting the existence of mechanism-based sirtuin activating compounds (MB-STACs) that operate according to the mechanisms presented.

## Results

### Steady-state sirtuin kinetic modeling



409  
410  
411  
412  
413  
414  
415  
416  
417  
418  
419  
420  
421  
422  
423  
424  
425  
426  
427  
428  
429  
430  
431  
432  
433  
434  
435  
436  
437  
438  
439  
440  
441  
442  
443  
444  
445  
446  
447  
448  
449  
450  
451  
452  
453  
454  
455  
456  
457  
458  
459  
460  
461  
462  
463  
464  
465  
466  
467  
468  
469  
470  
471  
472  
473  
474  
475  
476

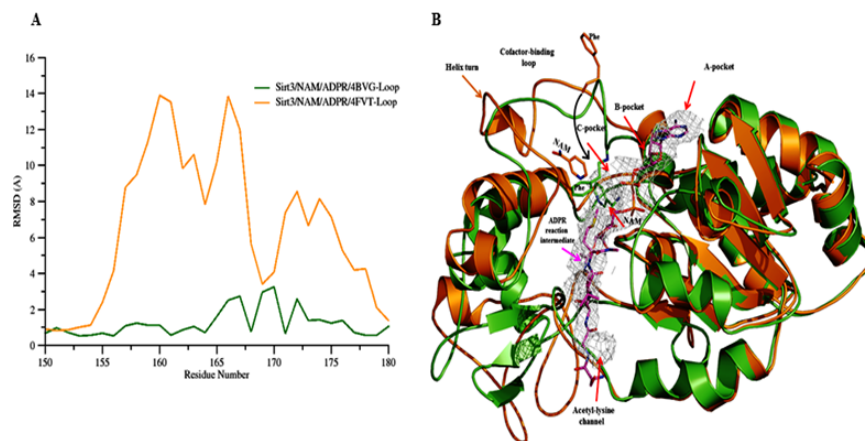


**Fig. 6.** Per-residue RMSD comparison for cofactor binding loop region. (A) Per-residue RMSD values for the cofactor binding loop region calculated using the MD averaged structure of Sirt3: ADPR: NAM complex modeled using the loop coordinates obtained from 4BVG (Green) and 4FVT (Orange). Crystal structure of a Sirt3 intermediate complex (4BVG) was used as the reference structure. Residues (162-170) form a short alpha helix when bound to co-factors. (B) Superposition of the time averaged MD structures of Sirt3/ADPR/NAM intermediate complex modelled based on the crystal structure of Sirt3 ternary complex (4FVT- orange) and another with the co-factor binding loop residues (155-178) being replaced from a native intermediate structure (4BVG–green). Differences in the conformations of the co-factor binding loop and the position of the Phe residue and NAM are highlighted. Individual subsites are highlighted; ADPR intermediate is rendered in sticks (carbons in Magenta) and NAM also shown in stick representation (Carbon atoms colored based on their respective protein cartoon color). A short helix is evident in Sirt3/ADPR/NAM intermediate complex modelled using 4FVT (Ternary complex), but not in the complex modelled using the co-factor binding loop replaced from the 4BVG (Native intermediate).

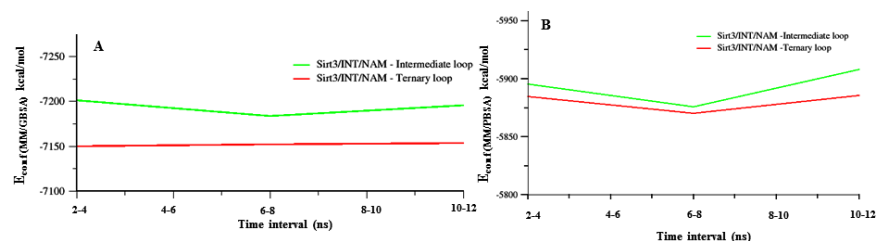


**Fig. 7.** Conformational energies of Sirt3-INT-NAM complexes. Conformational energies estimated using MM/PBSA and MM/GBSA method showing the energy gap for the Sirt3/INT/NAM complexes with different cofactor loop conformation. SIRT3/INT/NAM prepared from 4FVT with loop residues (res 155-178) replaced from 4FVT is shown in green and SIRT3/INT/NAM prepared from 4FVT with its native loop is shown in red. Panel A shows a plot of MM/GBSA conformational energy vs time and B shows plot of MM/PBSA vs times for the two different conformers.

**Table 1. Conformation energy differences and binding energy difference for Sirt3 intermediate complex with different loop conformation calculated using calculated with the MM/PBSA and MM/GBSA method. Energy values are reported in kcal/mol.**

Conformational energy difference of the Sirt3 intermediate complex			
Energy components for the complex	$\Delta G_A$ (SIRT3/INT/NAM prepared from 4FVT)	$\Delta G_B$ SIRT3/INT/NAM prepared from 4FVT with loop (res 155-178) replaced from 4BVG	$\Delta \Delta G_{(B \rightarrow A)}$ and $\Delta \Delta_{BE (B \rightarrow A)}$
$\langle E_{MM/GBSA} \rangle$	$-7146.48 \pm 3.55$	$-7201.58 \pm 3.44$	<b>-55.10</b>
$\langle E_{MM/PBSA} \rangle$	$-5873.69 \pm 3.87$	$-5901.23 \pm 3.76$	<b>-27.54</b>
$\Delta_{BE (MM/GBSA)} (\Delta E_{Complex} - \Delta E_{Receptor} - \Delta E_{Ligand})$	$-20.33 \pm 0.13$	$-22.50 \pm 0.13$	<b>-2.17</b>
$\Delta_{BE (MM/PBSA)} (\Delta E_{Complex} - \Delta E_{Receptor} - \Delta E_{Ligand})$	$-3.96 \pm 0.25$	$-7.73 \pm 0.26$	<b>-3.77</b>

\*  $\langle \rangle$  signifies ensemble average values computed from MD trajectories. The standard errors ( $\pm$ ) for the values are also provided.  $\langle E_{MM/GBSA} \rangle$  and  $\langle E_{MM/PBSA} \rangle$  signifies the conformational energies of the Sirt3-INT-NAM complex.  $\Delta_{BE (MM/GBSA)}$  and  $\Delta_{BE (MM/PBSA)}$  signifies the binding energy of NAM for Sirt3.  $\Delta \Delta G_{B \rightarrow A}$  signifies the conformational energy differences between two conformational states (B and A) which vary in the cofactor loop conformation.  $\Delta \Delta_{BE (B \rightarrow A)}$  quantifies the relative binding energy difference of NAM for Sirt3 between two conformational loop conformations (B and A).

To a greater extent than inhibitor design, rational activator design requires the use of a mechanistic model in the workflow. In this section we develop a steady state model for sirtuin-catalyzed deacylation that is suitable for a) investigation of the mode of action of mechanism-based sirtuin modulators, including activators; b) design of mechanism-based sirtuin activating compounds.

We first summarize the state of knowledge regarding the sirtuin-catalyzed deacylation mechanism.

The sirtuin catalytic cycle (Fig. 1) is believed to proceed in two consecutive stages [4]. The initial stage (ADP-ribosylation) involves the cleavage of the nicotinamide moiety of  $NAD^+$  and the nucleophilic attack of the acyl-Lys side chain of the protein substrate to form a positively charged O-alkylimidate interme-

477  
478  
479  
480  
481  
482  
483  
484  
485  
486  
487  
488  
489  
490  
491  
492  
493  
494  
495  
496  
497  
498  
499  
500  
501  
502  
503  
504  
505  
506  
507  
508  
509  
510  
511  
512  
513  
514  
515  
516  
517  
518  
519  
520  
521  
522  
523  
524  
525  
526  
527  
528  
529  
530  
531  
532  
533  
534  
535  
536  
537  
538  
539  
540  
541  
542  
543  
544

545  
546  
547  
548  
549  
550  
551  
552  
553  
554  
555  
556  
557  
558  
559  
560  
561  
562  
563  
564  
565  
566  
567  
568  
569  
570  
571  
572  
573  
574  
575  
576  
577  
578  
579  
580  
581  
582  
583  
584  
585  
586  
587  
588  
589  
590  
591  
592  
593  
594  
595  
596  
597  
598  
599  
600  
601  
602  
603  
604  
605  
606  
607  
608  
609  
610  
611  
612

diolate [4, 24]. Nicotinamide-induced reversal of the intermediate (the so-called base exchange reaction) causes reformation of NAD<sup>+</sup> and acyl-Lys protein. The energetics of this reversible reaction affects both the potency of NAM inhibition of sirtuins and the Michaelis constant for NAD+ (K<sub>m,NAD+</sub>). The second stage of sirtuin catalysis, which includes the rate-determining step, involves four successive steps that culminate in deacylation of the Lys side chain of the protein substrate and the formation of O-acetyl ADP ribose coproduct [4, 6, 25, 26].

A tractable steady state model suitable for the purpose of mechanism-based sirtuin activator design must account for the following important features:

- The calculated free energy of activation for nicotinamide cleavage (ADP-ribosylation of the acyl-Lys substrate) in the bacterial sirtuin enzyme Sir2Tm as computed through mixed quantum/molecular mechanics (QM/MM) methods is 15.7 kcal mol<sup>-1</sup> [27]. An experimental value of 16.4 kcal mol<sup>-1</sup> for the activation barrier in the yeast sirtuin homolog Hst2 was estimated from the reaction rate 6.7 s<sup>-1</sup> of nicotinamide formation [25]. The nicotinamide cleavage reaction is endothermic, with a computed ΔG of 4.98 kcal mol<sup>-1</sup> in Sir2Tm [27].

- The calculated free energy of activation for the rate limiting chemistry step (collapse of the bicyclic intermediate) from QM/MM simulations is 19.2 kcal mol<sup>-1</sup> for Sir2Tm [28], in good agreement with the experimental value of 18.6 kcal/mol<sup>-1</sup> estimated from the k<sub>cat</sub> value of 0.170 ± 0.006 s<sup>-1</sup> [29] (0.2 +/- 0.03 s<sup>-1</sup> for Hst2 [25]).

- The remaining steps in the catalytic cycle are significantly faster than the above steps. The other chemistry steps in stage 2 of the reaction are effectively irreversible [28], as is product release in the presence of saturating peptide concentrations.

We hence include in our kinetic model representations of all steps in stage 1 of the reaction, including the nicotinamide cleavage/base exchange and nicotinamide binding steps. However, for simplicity, we do not include in the present model a representation of each of the individual chemistry steps in stage 2 of the reaction or final product release, instead subsuming these steps under the smallest rate constant, which we call k<sub>cat</sub>. Since all these steps are effectively irreversible, the full steady state model including these steps can be immediately derived from the basic model through simple modifications, to be described in a subsequent revision, that are not essential to the analysis of mechanism-based activation. The above observations motivate the kinetic model represented in Fig. 2 [30]. This Figure shows a general reaction scheme for sirtuin deacylation including base exchange inhibition.

The reaction mechanism of sirtuins precludes the use of rapid equilibrium methods for the derivation of even an approximate initial rate model; steady-state modeling is essential. The rate equations for the reaction network in Fig. 2 enable the derivation of steady-state conditions for the reaction. Solving the linear system of algebraic steady-state equations and mass balance constraints for the concentrations

$$[E.Ac-Pr], [E.Ac-Pr.NAD^+], [E.ADP-Pr.Ac-Im.NAM], [E.ADP-Pr.Ac-Im], [E.NAM]$$

in terms of the rate constants and [NAD+],[NAM], which are assumed to be in significant excess and hence approximately equal to their initial concentrations [NAD+]<sub>0</sub>, [NAM]<sub>0</sub> respectively, we obtain expressions of the form (1):

$$\begin{aligned} [E.Ac-Pr]/[E]_0 &= c_{11} + c_{12}[NAM] \\ [E.Ac-Pr.NAD^+]/[E]_0 &= c_{21}[NAD^+] + c_{22}[NAD^+][NAM] \\ [E.ADP-Pr.Ac-Im.NAM]/[E]_0 &= c_{31}[NAD^+] + c_{32}[NAD^+][NAM] \\ [E.ADP-Pr.Ac-Im]/[E]_0 &= c_{41}[NAD^+] \\ [E.Ac-Pr.NAM]/[E]_0 &= c_{51}[NAD^+] + c_{52}[NAM] + c_{53}[NAD^+][NAM] + c_{54}[NAM]^2 \end{aligned} \quad (1)$$

Where, the term c<sub>54</sub> that is second order in [NAM] will be omitted from the analysis below. Expressions for the c<sub>ij</sub>'s are provided in the Appendix. The initial rate of deacylation can be then expressed

$$v = \frac{[NAD^+] \left( 1 + \frac{[NAM]}{K_1} \right)}{K_{m,NAD^+} \left( 1 + \frac{[NAM]}{K_2} \right) + [NAD^+] \left( 1 + \frac{[NAM]}{K_3} \right)} \quad (2)$$

With

$$\begin{aligned} v_{max} &= \frac{k_{cat} k_1 k_2 k_3 (k_2 + k_{cat})}{k_2 k_1 k_2 k_2 + k_{cat} (k_2 k_{cat} k_1 + k_2 k_2 k_1 + k_2 k_1 k_{cat} + k_2 k_1 k_{cat} + k_1 k_2 k_{cat})} [E]_0 \\ &\approx k_{cat} [E]_0 \\ K_{m,NAD^+} &= \frac{k_{cat} k_2 [k_{ex} k_{cat} + k_1 k_{cat} + k_{ex} k_2 + k_3 k_2 + k_{ex} k_1]}{k_2 k_1 k_2 k_2 + k_{cat} (k_2 k_{cat} k_1 + k_2 k_2 k_1 + k_2 k_1 k_{cat} + k_2 k_1 k_{cat} + k_1 k_2 k_{cat})} \\ &\approx k_{cat} \frac{k_{ex} k_2 + k_1 (k_2 + k_{cat})}{k_1 k_2 k_2} = k_{cat} \left( \frac{1}{k_1} + K_{d,NAD^+} \frac{k_2 + k_{cat}}{k_2 k_2} \right) \\ \frac{1}{K_1} &= \frac{k_1}{k_2 + k_{cat}} \approx \frac{1}{K_{d,NAD^+}} \quad (3a-e) \\ \frac{1}{K_2} &= \frac{1}{K_{m,NAD^+}} \frac{k_2 k_{cat} k_3 (k_2 + k_{cat}) + k_{cat} (k_2 k_{cat} k_1 + k_2 k_2 k_1 + 2k_2 k_1 k_{cat} + 2k_2 k_1 k_2)}{k_2 k_1 k_2 k_2 + k_{cat} (k_2 k_{cat} k_1 + k_2 k_2 k_1 + k_2 k_1 k_{cat} + k_2 k_1 k_{cat} + k_1 k_2 k_{cat})} \approx \frac{K_{d,NAD^+} K_{ex}}{K_{m,NAD^+} K_{d,NAD^+}} \\ \frac{1}{K_3} &\approx \frac{1}{\alpha K_1} = \frac{k_1 k_2 k_3 (k_{ex} + k_{cat}) + k_{cat} k_2 k_3 (k_2 + k_{cat})}{k_2 k_1 k_2 k_2 + k_{cat} (k_2 k_{cat} k_1 + k_2 k_2 k_1 + k_2 k_1 k_{cat} + k_2 k_1 k_{cat} + k_1 k_2 k_{cat})} \approx \frac{1 + K_{ex}}{K_{d,NAD^+}} \end{aligned}$$

Where K<sub>ex</sub> ≡ k<sub>-ex</sub>/k<sub>ex</sub> and the approximations refer to the case where

$$k_{cat} \square k_j, j \neq cat$$

Equation (2) is typically represented graphically in terms of either double reciprocal plots at constant [NAM] or Dixon plots at constant [NAD+]. In the former case, the slope of the plot (1/v vs 1/[NAD+]) at [NAM]=0 is K<sub>m,NAD+</sub>/v<sub>max</sub>, for which the expression is:

$$\frac{K_{m,NAD^+}}{v_{max}} \approx \frac{1}{[E]_0} \left( \frac{1}{k_1} + K_{d,NAD^+} \frac{k_2 + k_{cat}}{k_2 k_2} \right) \approx \frac{K_{m,NAD^+}}{k_{cat} [E]_0} \quad (4)$$

- Catalytic efficiency of sirtuins cannot be improved by increasing k<sub>cat</sub>. Hence was not important to include rep of stage 2 of reaction in model

whereas for the Dixon plot, the expression for the slope at 1/[NAD+]=0 is approximately [30]:

$$\frac{1}{K_3} \frac{1}{v_{max}} \approx \frac{1 + K_{ex}}{K_{d,NAD^+}} \frac{1}{k_{cat} [E]_0} \quad (5)$$

The steady state parameter α in equation (3e), which is a measure of the extent of competitive inhibition by the endogeneous inhibitor NAM against the cofactor NAD+, can be expressed in terms of the ratio of K<sub>d,NAD+</sub> and K<sub>m,NAD+</sub> [29]:

681  
682  
683  
684  
685  
686  
687  
688  
689  
690  
691  
692  
693  
694  
695  
696  
697  
698  
699  
700  
701  
702  
703  
704  
705  
706  
707  
708  
709  
710  
711  
712  
713  
714  
715  
716  
717  
718  
719  
720  
721  
722  
723  
724  
725  
726  
727  
728  
729  
730  
731  
732  
733  
734  
735  
736  
737  
738  
739  
740  
741  
742  
743  
744  
745  
746  
747  
748

$$\alpha = \frac{K_2}{K_2} \approx \frac{K_{d,NAD+}}{K_{m,NAD+}} \frac{K_{ex}}{1 + K_{ex}} \quad (6)$$

which, together with expression (3b) for  $K_{m,NAD+}$ , demonstrates how the kinetics of inhibition of deacylation by NAM can reveal differences in  $NAD^+$  binding affinity and nicotinamide cleavage rates among sirtuins. The origins of different  $NAD^+$  binding affinities among sirtuins were studied structurally and computationally in [30]. Given that  $K_{ex}$  is generally  $\gg 1$  for sirtuins, it is apparent from eqn (6) that the difference in magnitudes of  $K_{d,NAD+}$  and  $K_{m,NAD+}$  for sirtuins is captured by  $\alpha$ .  $K_{m,NAD+}$ , not  $K_{d,NAD+}$  alone, determines the sensitivity of sirtuin activity to  $NAD^+$ , and can vary across this family of enzymes. The initial rate model and the definition of  $\alpha$  allow  $K_{d,NAD+}$  to be estimated (under suitable approximations) by steady state deacylation experiments that vary [NAM] as well as [NAD+].

In addition to the approximation  $k_{cat} \square k_j, j \neq cat$ , several experimental observations can further simplify the form of the expressions (4) for the sirtuin steady state constants. First, we assume  $k_{-2} \gg k_j, j \neq -2$  based on viscosity measurements that suggest NAM dissociates rapidly following cleavage [30]. Under this approximation, the expression for  $K_{m,NAD+}$  becomes:

$$K_{m,NAD+} \approx k_{cat} \left( \frac{1}{k_1} + \frac{K_{d,NAD+}}{k_{ex}} \right) \quad (7)$$

The magnitudes of the on/off rates for  $NAD^+$  binding also affect the accuracy of approximations to equations (2,3). Such approximations will be studied in greater detail in a subsequent work.

As can be seen from eqn (3b), the kinetics of the nicotinamide cleavage reaction and the rate limiting step of deacylation both play essential roles in determining the value of  $K_{m,NAD+}$ . Note that in rapid equilibrium models of enzyme kinetics, which are not applicable to sirtuins,  $K_m \approx K_d$ . The difference between  $K_{d,NAD+}$  and  $K_{m,NAD+}$  has important implications for mechanism-based activation of sirtuins by small molecules [30]. In particular, as we will show in this work, decrease of  $K_{m,NAD+}$  independently of  $K_{d,NAD+}$  can increase the activity of sirtuins at [NAM] = 0. The kinetic model above establishes foundations for how this can be done.

### Mechanism-based sirtuin activation

Previous attempts to develop a general approach to sirtuin activation [31, 32] only considered competitive inhibitors of base exchange, which cannot activate in the absence of NAM. This is not actually a form of enzyme activation, but rather derepression of inhibition. By contrast, here we present paradigms and design criteria for activation of sirtuins in either the absence or presence of NAM. Based on expression (3b) for  $K_{m,NAD+}$ , it is in principle possible to activate sirtuins (not just SIRT1) for any substrate by alteration of rate constants in the reaction mechanism other than  $k_1, k_{-1}$  and  $k_{cat}$ , so as to reduce  $K_{m,NAD+}$  -- not  $K_{d,Ac-Pr}$  as with allosteric activators, which increase the peptide binding affinity of SIRT1 in a substrate-dependent fashion. We now explore how this may be achieved by augmenting the kinetic model to include putative mechanism-based activators (A) that can bind simultaneously with  $NAD^+$  and NAM. Fig. 3 depicts the reaction diagram for mechanism-based activation of sirtuins.

Note that only the top and front faces of this cube are relevant to the mechanism of action of the previously proposed competitive inhibitors of base exchange [31, 32].

At any [A] there exist apparent values of each of the rate constants in the sirtuin reaction mechanism. These are denoted by "app" in the Figure. There are also corresponding "app" values

of the steady state, Michaelis, and dissociation constants in equation (3). Moreover, at saturating [A] of a known activator, the modulated equilibrium and dissociation constants (which do not depend on determination of steady state species concentrations) can be estimated with only deacylation experiments according to the theory presented above. The exchange equilibrium constant  $K_{ex}'$  and  $NAD^+$ , NAM dissociation constants  $K_{d,NAD+}'$ ,  $K_{d,NAM}'$  in the presence of A are related to their original values as follows:

$$K_{d,NAD+}' = K_{d,NAD+} \frac{K_{d2,A}}{K_{d1,A}}; K_{ex}' = K_{ex} \frac{K_{d3,A}}{K_{d2,A}}; K_{d,NAM}' = K_{d,NAM} \frac{K_{d3,A}}{K_{d4,A}} \quad (8)$$

where the  $K_{d,i,A}$ 's are the dissociation constants for A depicted in Fig. 3.

In order to predict the effect on  $K_{m,NAD+}^{app}$  of a modulator with specified relative binding affinities for the complexes in the sirtuin reaction mechanism, it is important to develop a model that is capable of quantifying, under suitable approximations, the effect of such a modulator on the apparent steady state parameters of the enzyme. Since the full steady state expression relating the original to the apparent rate constants has many terms containing products of additional side and back face rate constants, we use a rapid equilibrium segments approach to arrive at simple definitions of the apparent Michaelis constant and other steady state constants for the reaction in terms of the original expressions for these constants and the dissociation constants for binding of A to the various complexes in the sirtuin reaction mechanism. This provides a minimal model with the least number of additional parameters required to model sirtuin activation mechanisms. In our treatment, we will assume that rapid equilibrium applies on both the side faces and the back face. Under this approximation, at low [A] the expressions for the induced changes in each of the rate constant products appearing in the coefficients  $c_{ij}$  and  $c_{ij}'$ ,  $i'=i$  of equation (1) (see Appendix for expressions for these products) are the same and linear in [A]. For example, in the case of  $E_{Ac-Pr}$ , the steady state species concentrations become:

$$\begin{aligned} [E_{Ac-Pr}] / [E_{Ac-Pr}]_0 &\approx c_{11} + c_{12} [NAM] \\ [E_{Ac-Pr} \cdot A] / [E_{Ac-Pr}]_0 &\approx \frac{[A]}{K_{d1,A}} (c_{11} + c_{12} [NAM]) \end{aligned} \quad (9)$$

The rapid equilibrium segments expressions for all species concentrations in equation (1) in the presence of A are provided in the Appendix.

Expressions for apparent values of all steady state parameters introduced in equation (3) (i.e., modulated versions of constants  $v_{max}, K_{m,NAD+}, K_1, K_2, K_3$ ) in the presence of a given [A] can now be derived. In the following, several types of approximations will be invoked:

- i: rapid equilibrium segments approximation
- ii:  $k_{cat} (1 + K_{d,l,A}) \square k_j (1 + K_{d,l,A}), j \neq cat, l = 1, \dots, 5$
- iii:  $k_{-2} (1 + K_{d,l,A}) \square k_j (1 + K_{d,l,A}), j \neq -2, l = 1, \dots, 5$  (rapid NAM dissociation)

$$\frac{v_{m,app}}{[E]_0} = \frac{k_{cat,app} (c_{31,app} + c_{41,app})}{c_{21,app} + c_{31,app} + c_{41,app} + c_{51,app}}$$

$$K_{m,app} = \frac{k_{cat} (k_{11} k_2 k_3 (1 + [A]/K_{d1,A}) + k_1 k_2 k_3 (1 + [A]/K_{d1,A}))}{k_{cat} (k_2 k_3 + k_2 k_3 + k_2 k_3) (1 + [A]/K_{d1,A}) + k_{cat} k_2 k_3 (1 + [A]/K_{d1,A}) + k_1 k_2 k_3 (1 + [A]/K_{d1,A}) + k_{cat} k_2 k_3 (1 + [A]/K_{d1,A})}$$

$$\approx \frac{k_{cat} c_{41} (1 + [A]/K_{d4,A})}{c_{41} (1 + [A]/K_{d4,A})} \approx k_{cat} \approx k_{cat,app} \quad (10)$$



817  
818  
819  
820  
821  
822  
823  
824  
825  
826  
827  
828  
829  
830  
831  
832  
833  
834  
835  
836  
837  
838  
839  
840  
841  
842  
843  
844  
845  
846  
847  
848  
849  
850  
851  
852  
853  
854  
855  
856  
857  
858  
859  
860  
861  
862  
863  
864  
865  
866  
867  
868  
869  
870  
871  
872  
873  
874  
875  
876  
877  
878  
879  
880  
881  
882  
883  
884

$$K_{m,NAD^+,app} = \frac{c_{11,app}}{c_{21,app} + c_{31,app} + c_{41,app} + c_{51,app}}$$

$$\approx \frac{c_{11} \left( 1 + \frac{[A]}{K_{d1,A}} \right)}{c_{21} \left( 1 + \frac{[A]}{K_{d2,A}} \right) + c_{31} \left( 1 + \frac{[A]}{K_{d3,A}} \right) + c_{41} \left( 1 + \frac{[A]}{K_{d4,A}} \right) + c_{51} \left( 1 + \frac{[A]}{K_{d5,A}} \right)}$$

$$\approx k_{cat} \left( \frac{1}{k_1} + \frac{K_{d,NAD^+}}{k_{cat}} \right) \frac{1 + [A]/K_{d1,A}}{1 + [A]/K_{d1,A}} \approx k_{cat,app} \left( \frac{1}{k_1} + \frac{K_{d,NAD^+,app}}{k_{cat,app}} \right) \frac{1 + [A]/K_{d1,A}}{1 + [A]/K_{d1,A}} \quad (11)$$

$$\approx k_{cat,app} \left( \frac{1}{k_1,app} + \frac{K_{d,NAD^+,app}}{k_{cat,app}} \right)$$

Recall that  $\alpha$  provides an estimate of the ratio of the dissociation and Michaelis constants for  $NAD^+$ .

$$\alpha_{app} \approx \frac{c_{12}(1+[A]/K_{d1,A}) + c_{32}(1+[A]/K_{d3,A})}{c_{22}(1+[A]/K_{d2,A}) + c_{32}(1+[A]/K_{d3,A}) + c_{53}(1+[A]/K_{d5,A})} \frac{1}{K_{m,NAD^+,app}} \quad (12)$$

$$\approx \frac{K_{d,NAD^+}}{K_{m,NAD^+}} \frac{K_{ex}}{1+K_{ex}} \frac{(1+[A]/K_{d4,A})}{(1+[A]/K_{d2,A})} \approx \frac{K_{d,NAD^+,app}}{K_{m,NAD^+,app}} \frac{K_{ex,app}}{1+K_{ex,app}}$$

$$\alpha_{app}^{K_{m,NAD^+,app}} \approx K_{d,NAD^+} \frac{K_{ex}}{1+K_{ex}} \frac{(1+[A]/K_{d1,A})}{(1+[A]/K_{d2,A})} \approx K_{d,NAD^+,app} \frac{K_{ex,app}}{1+K_{ex,app}} \quad (13)$$

The latter provides an estimate of  $K_{d,NAD^+,app}$  if  $K_{ex} \ll 1$ , as it is believed to be for most sirtuins.

Under approximation (ii),  $K_3$  isolates nicotinamide cleavage / base exchange-specific effects.

$$\frac{1}{K_{3,app}} \approx \frac{c_{22}(1+[A]/K_{d2,A}) + c_{32}(1+[A]/K_{d3,A}) + c_{53}(1+[A]/K_{d5,A})}{c_{21}(1+[A]/K_{d2,A}) + c_{31}(1+[A]/K_{d3,A}) + c_{41}(1+[A]/K_{d4,A}) + c_{51}(1+[A]/K_{d5,A})} \quad (14)$$

$$\approx \frac{1+K_{ex}}{K_{d,NAD^+}} \frac{(1+[A]/K_{d2,A})}{(1+[A]/K_{d4,A})} \frac{1+K_{ex,app}}{K_{d,NAD^+,app}}$$

$$\frac{1}{K_{2,app}} = \frac{c_{12,app} + c_{52,app}}{c_{11,app}} \approx \frac{c_{12}(1+[A]/K_{d1,A}) + c_{52}(1+[A]/K_{d5,A})}{c_{11}(1+[A]/K_{d1,A})}$$

$$\approx \frac{c_{12}(1+[A]/K_{d1,A})}{c_{11}(1+[A]/K_{d1,A})} = \frac{K_{d,NAD^+} K_{ex}}{K_{m,NAD^+} K_{d,NAM}} \approx \frac{K_{d,NAD^+,app} K_{ex,app}}{K_{m,NAD^+,app} K_{d,NAM,app}} \quad (15)$$

Regarding the quality of the approximations in this case, note from (15) and (A1) that unlike any of the other steady-state parameters, the modulation  $\frac{1}{K_{2,app}} - \frac{1}{K_2}$  induced by [A] is proportional to  $k_{cat}$  under the rapid equilibrium segments approximation (first approximation above). Hence, if one is interested in estimating the sign of this modulation, the small  $k_{cat}$  approximation (second approximation above) should not be applied. Also, under the rapid equilibrium segments approximation,  $K_{2,app}$  is the only constant that relies on a ratio of two  $c_{ij}$ 's with  $i=i, j' \neq j$ , and hence the ratio of the same factor in [A]. It is obvious that the apparent values of rate constant products in the numerator and

denominator above cannot be precisely equal and hence  $K_{2,app}$  will have to change slightly from  $K_2$ .

$$\frac{1}{K_{1,app}} = \frac{c_{32,app}}{c_{31,app} + c_{42,app}}$$

$$\approx \frac{k_1 k_{cat} k_2 k_{-2} (1+[A]/K_{d3,A})}{k_{cat} k_1 k_2 k_{-2} (1+[A]/K_{d3,A}) + k_1 k_{cat} k_2 k_{-2} (1+[A]/K_{d4,A})}$$

$$\approx \frac{1}{K_{d,NAM}} \frac{1+[A]/K_{d3,A}}{1+[A]/K_{d4,A}} \quad (16)$$

### Conditions for mechanism-based activation

We now consider thermodynamic conditions on the binding of a modulator A for mechanism-based sirtuin activation under the rapid equilibrium segments approximation, along with the expected changes in the steady state, equilibrium and dissociation constants in the sirtuin reaction mechanism.

First, according to equation (10),  $v_{max}/[E]_0$  is roughly unchanged within this family of mechanisms as long as the  $K_{d,A}$ 's for [A] binding to the various represented complexes in the reaction mechanism satisfy condition (iii). Thus, enzyme activation is expected if  $K_{m,NAD^+,app}$  can be decreased relative to  $K_{m,NAD^+}$  - i.e., if the sensitivity of sirtuins to  $NAD^+$  can be increased. According to equation (11),  $K_{m,NAD^+,app}$  will be smaller than  $K_{m,NAD^+}$  if  $K_{d1,A}/K_{d4,A} \geq (K_{d1,A}/K_{d2,A})(K_{d2,A}/K_{d3,A})(K_{d3,A}/K_{d4,A}) > 1$ . To identify mechanisms by which this can occur in terms of the steps in the sirtuin-catalyzed reaction, we consider in turn each of these three respective ratios of  $K_{d,A}$ 's (or equivalently, the  $\Delta\Delta G^\ddagger$ 's of the  $NAD^+$  binding, exchange, and NAM binding reactions as implied by equation (8)) induced by A binding.

According to equation (13),  $K_{d1,A}/K_{d2,A} < 1$  would imply that A binding increases the binding affinity of  $NAD^+$  to the E.Ac-Pr complex. This is biophysically implausible for mechanism-based activation; when dissociation constants for substrates decrease upon small molecule binding, this typically occurs through an allosteric mechanism.

Comparison of the crystal structure of human Sirt3/AcS2 peptide/Carba  $NAD^+$  ternary complex (4FVT) with Sirt3 apo structure (3GLS) shows the cofactor binding loop adapts a close-to-ternary loop conformation (See Fig 4 and Supporting Information --). 3GLS (apo structure) has close-to-ternary loop conformation (See Fig 4 and Supporting Information)

This means that it will be difficult to preferentially stabilize the ternary complex relative to the apo complex using a modulator.

In particular, this renders  $K_{d,NAD^+}$  reduction more challenging than other types of  $K_{m,NAD^+}$  reduction.

Thus, we assume that for a mechanism-based activator,  $K_{d1,A} \geq K_{d2,A}$ . Then, in order to have  $K_{m,NAD^+,app} < K_{m,NAD^+}$ , we require  $(K_{d2,A}/K_{d3,A})(K_{d3,A}/K_{d4,A}) > K_{d1,A}/K_{d2,A}$  or equivalently, according to (8),  $(K_{d,NAM}/K_{ex})(K_{ex}/K_{d,NAM}) > K_{d,NAD^+}/K_{d,NAD^+}$ . The decrease in  $K_{m,NAD^+}$  can hence be due to modulation of the exchange rate constants that induces a decrease in  $K_{ex}$ , an increase in  $K_{d,NAM}$ , or both. We assume  $K_{d,NAM}' \geq K_{d,NAM}$  ( $K_{d3,A} \geq K_{d4,A}$ ) for reasons analogous to those for  $K_{d,NAD^+}$  (NAM being the nicotinamide moiety of  $NAD^+$ ). This corresponds to mixed noncompetitive inhibition [30] of base exchange.

As we have previously shown [30], the nicotinamide moiety of  $NAD^+$  engages in nearly identical interactions with the enzyme before and after bond cleavage. The salient difference is a conformational change in a conserved phenylalanine side chain (e.g., Phe33 in Sir2Tm, Phe157 in SIRT3) that destabilizes NAM binding after bond cleavage [33, 34].

953  
954  
955  
956  
957  
958  
959  
960  
961  
962  
963  
964  
965  
966  
967  
968  
969  
970  
971  
972  
973  
974  
975  
976  
977  
978  
979  
980  
981  
982  
983  
984  
985  
986  
987  
988  
989  
990  
991  
992  
993  
994  
995  
996  
997  
998  
999  
1000  
1001  
1002  
1003  
1004  
1005  
1006  
1007  
1008  
1009  
1010  
1011  
1012  
1013  
1014  
1015  
1016  
1017  
1018  
1019  
1020

Since NAM binding is already destabilized by the native protein conformation in this way, and since  $\Delta\Delta G_{\text{bind,NAD}^+}$  induced by the modulator will generally be greater in magnitude than  $\Delta\Delta G_{\text{bind,NAM}}$  due to disruption of additional contacts between the ADPR moiety of NAD<sup>+</sup> and the enzyme,  $\frac{K_{d2,A}}{K_{d3,A}}$  is likely to make the dominant contribution to  $\frac{K_{d2,A}}{K_{d4,A}}$ .

Note that there is ample scope for modulation of  $\Delta G_{\text{e}}$  by the modulator due to the coupling of the endothermic nicotinamide cleavage / ADP ribosylation reaction (exothermic base exchange reaction) to a conformational change in the sirtuin cofactor binding loop.  $\Delta G_{\text{e}}$  for Sir2Tm has been calculated to be -4.98 kcal/mol [27]. (For comparison,  $\Delta G_{\text{bind,NAM}}$  for Sir2Af2 was estimated to be -4.1 kcal/mol [31] and  $\Delta G_{\text{bind,NAM}}$  for SIRT3 was estimated to be  $\leq -3.2$  kcal/mol [30].) Tighter binding of modulators to the intermediate (ADPR-Pr-Im) complex compared to ternary substrate (NAD<sup>+</sup>, peptide)-bound complex is possible due to the fact that this substantial conformational rearrangement of sirtuin loops occurs universally upon NAM cleavage [34]. The flexible loop in 4BVG (intermediate complex) has a significantly higher RMSD with respect to that in 4FVT (ternary complex) than does the flexible loop in 3GLS (apo-enzyme). Hence it is plausible that the intermediate complex can bind more tightly to the ligand than the substrate complex through such flexible loop interactions. Across all sirtuins studied, nicotinamide cleavage induces similar structural changes (for example, unwinding of a helical segment in the flexible cofactor binding loop [33, 34]; see Fig 5 and Supporting Information ---) and such changes might enable preferential stabilization of the E.ADPR-Pr-Im complex, in a manner similar to the stabilization of specific loop conformations by mechanism-based inhibitors [18].

Note that sirtuin ELT inhibitors [35], which are peptidomimetics that also extend into the C pocket (through a NAM-mimicking moiety), induce a 4BVG (ADPR-Pr-Im complex)-like loop conformation with a similar alpha turn and without the helix that is present in the ternary loop conformation (See fig 4).

This suggests that modulators (if they do not compete with substrates) can induce the desired loop conformational changes / stabilization of ADPR-Pr-Im-like loop conformations.

Taken together, these observations suggest that  $\frac{K_{d2,A}}{K_{d3,A}} / \frac{K_{d3,A}}{K_{d4,A}} > \frac{K_{d2,A}}{K_{d4,A}}$  and that the value of  $\frac{K_{d2,A}}{K_{d4,A}}$  required for activation is likely to be achieved primarily by altering the free energy change of the nicotinamide cleavage reaction. However, our model accommodates the possibility of arbitrary combinations of  $\Delta\Delta G_{\text{e}}$  and  $\Delta\Delta G_{\text{bind,NAM}}$  contributing to activation.

Computational studies of the loop conformational change have not previously been reported. The closest prior study comprised QM/MM simulations of stage 2 of catalysis (starting from intermediate complex) [28]. In the present study MD simulations have been carried out on SIRT3/INT/NAM complex prepared from 4FVT with and without loop replacement that is taken from residue 155-178 of 4BVG.

Time averaged MD structure obtained revealed loss of structural stability for Sirt3/INT/NAM complex modeled using the ternary loop conformation (See fig 6 B). In addition the conformational energy of the complex as calculated using the Amber all-atom force field in conjunction with implicit solvent also suggest the complex to be energetically less stable in relation to the complex structure modeled using an loop conformation from an intermediate sirt3 complex.

Thus, we find that the following thermodynamic conditions on the binding of A to the various complexes in the sirtuin reaction mechanism are physically plausible and conducive to mechanism-based activation:

$$\begin{aligned} K_{d1,A} \leq K_{d2,A} &\Leftrightarrow K_{d,NAD^+} \geq K_{d,NAD} \\ K_{d2,A} \gg K_{d3,A} &\Leftrightarrow K_{\text{ex}} \ll K_{\text{on}} \\ K_{d3,A} \geq K_{d4,A} &\Leftrightarrow K_{d,NAM} \geq K_{d,NAM} \end{aligned} \quad (17)$$

where the  $\gg$  sign signifies that  $\frac{K_{d2,A}}{K_{d3,A}} > \frac{K_{d1,A}}{K_{d4,A}}$ . Finally, in our original model for sirtuin kinetics in Fig. 2, we assumed that both  $K_{d,NAM}$ 's – namely, those for dissociation of NAM from E.Ac-Pr.NAM and E.ADPR-Pr-Im.NAM – are roughly equal. We maintain this condition in the presence of A binding, which is reasonable given that A is assumed to not interact directly with the peptide or ADPR moiety, and since NAM binding does not rely on interactions with the flexible cofactor binding loop [26, 29]. Hence, we have:

$$\frac{[E.ADPR-Pr-Im][NAM]}{[E.ADPR-Pr-Im.NAM]} \approx \frac{[E.Ac-Pr][NAM]}{[E.Ac-Pr.NAM]} \Leftrightarrow K_{d5,A} \approx \frac{K_{d1,A}K_{d3,A}}{K_{d4,A}} \quad (18)$$

We now consider the effects of binding of a modulator A that satisfies the above requirements for activation on the remaining steady state constants.

-  $K_{\text{app}}$ : According to equation (12), the aforementioned requirement for activation that  $\frac{K_{d2,A}}{K_{d4,A}} \geq \frac{K_{d1,A}}{K_{d4,A}}$  implies a significant increase in  $\alpha$  by a factor that will generally exceed  $\frac{K_{m,NAD^+}}{K_{m,NAD^+,app}}$ .

-  $K_{3,app}$ : According to equation (14), in the presence of such a mechanism-based activator,  $K_3$  is expected to increase by a factor similar to that for  $\alpha$  under the rapid equilibrium segments approximation. This can occur due to an increase in  $K_{d,NAM}$ , decrease in  $K_{\text{ex}}$ , or both. Decrease in  $K_{\text{ex}}$  corresponds to hyperbolic (or partial) noncompetitive inhibition [30] of base exchange/activation of nicotinamide cleavage. With an additional increase in  $K_{d,NAM}$ , noncompetitive inhibition of base exchange becomes mixed noncompetitive inhibition of base exchange. Additional information (e.g., from high [NAM] initial rate experiments, which permit estimation of  $K_{d,NAM,app}$ ) is required to separate these possible causes.

-  $K_{2,app}$ : With conditions (17), equation (14) predicts a small increase in  $K_2$  since  $K_{d5,A} > K_{d1,A}$ .  $K_2$  increases to a smaller extent than  $K_3$ .

-  $K_{1,app}$ : With conditions (17), equation (16) predicts an increase in  $K_1$ .

A salient feature of this mechanism-based model for enzyme activation is that the intermediate reaction step is accelerated and made more thermodynamically favorable at expense of destabilization of substrate binding. Instead of competition with respect to NAM for binding, then, selective stabilization of the reaction intermediate through preferential binding to structural features unique to the intermediate – in particular, an altered flexible loop conformation – may be capable of activating sirtuins. Binding energy estimates computed using MM/PBSA and MM/GBSA method also reveal the transition state (TS) intermediate to have preferential binding towards Sirt3 with an intermediate co-factor loop conformation over a ternary loop conformation (See Table 1). The conformational energies of the complex show that Sirt3/Int/NAM complex with an intermediate co-factor loop conformation to be energetically more stable. In order for this to be possible, the free energy gap  $\Delta\Delta G$  between such protein conformations must be sufficiently large for  $K_{d3,A}/K_{d2,A}$  to be far enough from unity to produce a substantive change in the energetics of the reaction. In that case, according to the steady state model, selective stabilization of a loop conformation similar to that in the intermediate complex can have the net result of activation.

1021  
1022  
1023  
1024  
1025  
1026  
1027  
1028  
1029  
1030  
1031  
1032  
1033  
1034  
1035  
1036  
1037  
1038  
1039  
1040  
1041  
1042  
1043  
1044  
1045  
1046  
1047  
1048  
1049  
1050  
1051  
1052  
1053  
1054  
1055  
1056  
1057  
1058  
1059  
1060  
1061  
1062  
1063  
1064  
1065  
1066  
1067  
1068  
1069  
1070  
1071  
1072  
1073  
1074  
1075  
1076  
1077  
1078  
1079  
1080  
1081  
1082  
1083  
1084  
1085  
1086  
1087  
1088



1089 -Destabilization of secondary structure by ternary loop con-  
1090 formation in INT complex depicted above: consistent with MM-  
1091 GBSA results and suggests that there are destabilizing (unfavor-  
1092 able) interactions between INT and ternary loop

1093 Returning to equation (11) for  $K_{m,NAD^+}$  and  
1094 substituting  $(1+[A]/K_{d2,A})/(1+[A]/K_{d1,A}) \geq 1$ , the rapid equilibrium  
1095 assumptions applied to the present system imply that in order to  
1096 activate the enzyme at  $[NAM]=0$ , A must increase  $k_1$  ( $k_{1,app} > k_1$ ),  
1097  $k_{ex}$  ( $k_{ex,app} > k_{ex}$ ) or both. The rapid equilibrium segments  
1098 model is not able to distinguish between these scenarios, but  
1099 given that A is prone to increase  $K_{d,NAD^+}$ , assuming that it  
1100 also increases  $k_1$  is physically implausible. An increase in  $k_{ex}$   
1101 implies acceleration of the rate of nicotinamide cleavage. In  
1102 the rapid equilibrium segments framework, this occurs through  
1103 preferential stabilization of the E.ADPR-Pr-Im complex.

1104 We discuss below the biophysical underpinnings whereby an  
1105 increase in a forward rate constant could be achieved through  
1106 preferential stabilization of the intermediate complex.

#### 1107 *Potential means of increasing $k_{ex}$*

1108 From the standpoint of chemical mechanisms of activation,  
1109 the theory presented raises the important question of how the  
1110 nicotinamide cleavage rate  $k_{ex}$  of sirtuins can be accelerated by  
1111 a ligand that binds to the various complexes in the deacylation  
1112 reaction with the specified relative affinities, as predicted by  
1113 equation (11). It is important to note in this regard that the  
1114 nicotinamide cleavage reaction in sirtuins is generally believed  
1115 to be endothermic, which enables effective NAM inhibition of  
1116 the reaction [26, 36]. Unlike exothermic reactions, stabilization of  
1117 products or destabilization of reactants in endothermic reactions  
1118 can decrease the activation barrier for the forward reaction, due  
1119 to the fact that the transition state resembles the products more  
1120 than the reactants. The energetics of this reaction, including the  
1121 role of protein conformational changes, is being studied compu-  
1122 tationally in our group for mammalian sirtuins.

## 1123 Discussion

1124 We have presented a model for activation of sirtuin enzymes  
1125 suitable for the design and characterization of mechanism-based  
1126 sirtuin activating compounds (MB-STACs) that can in principle  
1127 activate any of the mammalian sirtuins SIRT1-7, unlike previously  
1128 proposed strategies for sirtuin activation. Also, the activation  
1129 model presented herein should be applicable to any substrate,  
1130 unlike previously reported allosteric activation of SIRT1 that was  
1131 found to accelerate deacylation for only a small fraction of over  
1132 6000 physiologically relevant peptide substrates studied, due to  
1133 the need for "substrate-assistance" in the allosteric mechanism  
1134 [13]. Moreover, this framework comprises a new mode of enzyme  
1135 activation that is distinct from any of the four modes of activation  
1136 previously known across all families of enzymes.

1137 Using this modeling framework, we have shown how modulation  
1138 of  $K_{m,NAD^+}$  independently of  $K_{d,NAD^+}$  can increase the activity of sirtu-  
1139 ins at  $[NAM]=0$  in a manner that mimics the effects of  $NAD^+$   
1140 supplementation [36] but in a selective fashion. This activation  
1141 also applies at nonzero  $[NAM]$ , decreasing the sensitivity of the  
1142 sirtuin to physiological NAM inhibition in addition to increasing  
1143 its sensitivity to physiological  $NAD^+$ . Such mechanism-based  
1144 sirtuin activation has advantages over a) allosteric activation,  
1145 which is only possible for SIRT1, is substrate-dependent, and  
1146 cannot fully compensate for the reduction in  $NAD^+$  levels that is  
1147 responsible for many aspects of health decline during organismic  
1148 aging [11, 12, 37]; b) activation of the  $NAD^+$  biosynthetic enzyme  
1149 Nampt [38], which regenerates  $NAD^+$  from NAM and hence has  
1150 nonselective effects on all enzymes that use an  $NAD^+$  cofactor;  
1151 and c) inhibition of  $NAD^+$ -dependent PARP enzymes, which  
1152 consume  $NAD^+$  but are required to repair DNA damage [23].

1153 Moreover, it has the potential to enable isoform-specific sirtuin  
1154 enzyme activation.

1155 The rapid equilibrium segments approximation (Appendix,  
1156 equation A3) was applied in order to illustrate how a ligand  
1157 that binds outside the  $NAD^+$  binding site can in principle in-  
1158 crease sirtuin activity through only modulation of the relative  
1159 free energies of the various species in the reaction mechanism.  
1160 More detailed analysis of the mechanism of action of MB-STACs  
1161 can be achieved by complete kinetic characterization in pres-  
1162 ence/absence of the activator (e.g., by coupling base exchange  
1163 with deacylation experiments). Such analyses will shed light on  
1164 whether mechanism-based sirtuin activation exploits the free  
1165 energy profile of the sirtuin nicotinamide cleavage and base  
1166 exchange reactions – and if so, how. Note that, as discussed, the  
1167 nicotinamide cleavage step is reversible and the DHP activator  
1168 both decreases the NAM sensitivity of the sirtuin and activates at  
1169  $[NAM]=0$ . Besides DHPs, it is worthwhile to apply the mecha-  
1170 nism identification methodology presented herein to any STACs  
1171 that may be found to activate either SIRT2-7 or SIRT1-catalyzed  
1172 reactions on substrates other than those of the limited type  
1173 identified in [11-13] to which traditional STACs are restricted.  
1174 The opportunities for mechanism-based activation of mammalian  
1175 sirtuins will depend on their particular values of  $K_{m,NAD^+}$  and the  
1176 underlying values of the associated rate constants. Importantly,  
1177 a sirtuin need not be highly sensitive to base exchange inhibition  
1178 in order to be susceptible to mechanism-based activation.

1179 Structurally, binding outside of the  $NAD^+$  binding site (the  
1180 so-called A and C pockets [26, 39]) appears to be essential for  
1181 mechanism-based activation. We are currently exploring prospec-  
1182 tive binding sites for MB-STACs. Moreover, rational design will  
1183 require analysis of the relative free energies of complexes de-  
1184 picted in Fig. 3. We have recently initiated computational studies  
1185 [30] that assess such free energy differences for some of the front  
1186 face (apo) complexes in this Figure, and further studies are in  
1187 progress.

1188 The enzyme activation theory presented herein motivates  
1189 experimental workflows for the hit identification, hit-to-lead evo-  
1190 lution, and lead optimization of mechanism-based activators. In  
1191 particular, the theory enables the identification and evolution of  
1192 important hits that may be inhibitors, not activators, by de-  
1193 composing the observed kinetic effects of a modulator into com-  
1194 ponents and identifying those molecules that display favorable  
1195 values of a subset of these components as hits even if the net  
1196 effect on catalytic turnover is inhibition. Compared to standard  
1197 library screening for hit identification and hit-to-lead evolution,  
1198 this approach allows application of multiobjective optimization  
1199 techniques (through iterative mutations to functional groups) to  
1200 sirtuin activator design. Such workflows would be fundamentally  
1201 different from traditional drug discovery workflows and would  
1202 bear more similarity to the directed evolution of enzymes. The  
1203 theory presented also establishes foundations for the rational  
1204 design of sirtuin-activating compounds, enabling the application  
1205 of state-of-the-art computational methods to activator design in a  
1206 manner analogous to computational enzyme design [40]. Finally,  
1207 it raises the important question as to whether other enzyme  
1208 families may also be activatable through such a mechanism-based  
1209 mode of action -- and if so, which families.

1210 The enzyme activation theory presented herein raises the  
1211 question as to whether other enzyme families may also be activat-  
1212 able through mechanism-based design-- and if so, which families.  
1213 Certainly, its application to other  $NAD^+$ -dependent enzymes,  
1214 such as poly- and mono ADP ribosyl transferases, should be con-  
1215 sidered. In principle, mechanism-based enzyme activation could  
1216 be used to selectively activate particular ADP ribosyl transferases,  
1217 increasing their sensitivity to  $NAD^+$  as its levels decline with age.  
1218 The potential diversity of the newly reported mode of mechanism-

1225  
1226  
1227  
1228  
1229  
1230  
1231  
1232  
1233  
1234  
1235  
1236  
1237  
1238  
1239  
1240  
1241  
1242  
1243  
1244  
1245  
1246  
1247  
1248  
1249  
1250  
1251  
1252  
1253  
1254  
1255  
1256  
1257  
1258  
1259  
1260  
1261  
1262  
1263  
1264  
1265  
1266  
1267  
1268  
1269  
1270  
1271  
1272  
1273  
1274  
1275  
1276  
1277  
1278  
1279  
1280  
1281  
1282  
1283  
1284  
1285  
1286  
1287  
1288  
1289  
1290  
1291  
1292

based enzyme activation far exceeds that of allosteric activation for such families of enzymes.

1. Kaeberlein M, McVey M, & Guarente L (1999) The SIR2/3/4 complex and SIR2 alone promote longevity in *Saccharomyces cerevisiae* by two different mechanisms. *Genes & Development* 13(19):2570-2580.
2. Hirsch BM & Zheng W (2011) Sirtuin mechanism and inhibition: explored with N(epsilon)-acetyl-lysine analogs. *Molecular bioSystems* 7(1):16-28.
3. Cen Y (2010) Sirtuins inhibitors: the approach to affinity and selectivity. *Biochimica et biophysica acta* 1804(8):1635-1644.
4. Sauve AA (2010) Sirtuin chemical mechanisms. *Biochimica Et Biophysica Acta-Proteins and Proteomics* 1804(8):1591-1603.
5. Hu P, Wang S, & Zhang Y (2008) Highly dissociative and concerted mechanism for the nicotinamide cleavage reaction in Sir2Tm enzyme suggested by ab initio QM/MM molecular dynamics simulations. *Journal of the American Chemical Society* 130(49):16721-16728.
6. Zhou Y, et al. (2012) The bicyclic intermediate structure provides insights into the desuccinylation mechanism of human sirtuin 5 (SIRT5). *The Journal of biological chemistry* 287(34):28307-28314.
7. Mercken EM, et al. (2014) SIRT2/104 extends survival of male mice on a standard diet and preserves bone and muscle mass. *Aging Cell* 13(5):787-796.
8. Mitchell SJ, et al. (2014) The SIRT1 activator SRT1720 extends lifespan and improves health of mice fed a standard diet. *Cell Rep* 6(5):836-843.
9. Zorn JA & Wells JA (2010) Turning enzymes ON with small molecules. *Nat Chem Biol* 6(3):179-188.
10. Sinclair DA & Guarente L (2014) Small-molecule allosteric activators of sirtuins. *Annual review of pharmacology and toxicology* 54:363-380.
11. Hubbard BP, et al. (2013) Evidence for a Common Mechanism of SIRT1 Regulation by Allosteric Activators. *Science* 339(6124):1216-1219.
12. Dai H, et al. (2015) Crystallographic structure of a small molecule SIRT1 activator-enzyme complex. *Nat Commun* 6:7645.
13. Lakshminarasimhan M, Rauh D, Schutkowski M, & Steegborn C (2013) Sirt1 activation by resveratrol is substrate sequence-selective. *Aging (Albany NY)* 5(3):151-154.
14. North BJ, et al. (2014) SIRT2 induces the checkpoint kinase BubR1 to increase lifespan. *Embo Journal* 33(13):1438-1453.
15. Brown K, et al. (2013) SIRT3 reverses aging-associated degeneration. *Cell Rep* 3(2):319-327.
16. Kanfi Y, et al. (2012) The sirtuin SIRT6 regulates lifespan in male mice. *Nature* 483(7388):218-221
17. Moniot S, et al (2012) Structures, Substrates, and Regulators of Mammalian Sirtuins – Opportunities and Challenges for Drug Development *Frontiers in Pharmacology*. 2012; 3: 16
18. Gertz M, et al. (2013) Ex-527 inhibits Sirtuins by exploiting their unique NAD(+) -dependent deacetylation mechanism. *Proceedings of the National Academy of Sciences of the United States of America* 110(30):E2772-E2781.
19. Rumpf T, et al. (2015) Selective Sirt2 inhibition by ligand-induced rearrangement of the active site. *Nat Commun* 6:6263.
20. Gomes AP, et al. (2013) Declining NAD(+) induces a pseudohypoxic state disrupting nuclear-mitochondrial communication during aging. *Cell* 155(7):1624-1638.
21. Qin WP, et al. (2006) Neuronal SIRT1 activation as a novel mechanism underlying the prevention of Alzheimer disease amyloid neuropathology by caloric restriction. *Journal of Biological Chemistry* 281(31):21745-21754.
22. Satoh A & Imai S (2014) Systemic regulation of mammalian ageing and longevity by brain sirtuins. *Nat Commun* 5:4211.
23. Massudi H, et al. (2012) Age-Associated Changes In Oxidative Stress and NAD(+) Metabolism In Human Tissue. *Plos One* 7(7):e42357.
24. Canto C, et al. (2012) The NAD(+) precursor nicotinamide riboside enhances oxidative metabolism and protects against high-fat diet-induced obesity. *Cell Metab* 15(6):838-847.
25. Smith BC & Denu JM (2007) Sir2 deacetylases exhibit nucleophilic participation of acetyl-lysine in NAD+ cleavage. *Journal of the American Chemical Society* 129(18):5802-5803.

## Computational Methodology

26. Avalos JL, Boeke JD, & Wolberger C (2004) Structural basis for the mechanism and regulation of Sir2 enzymes. *Molecular Cell* 13(5):639-648.
27. Liang Z, et al. (2010) Investigation of the catalytic mechanism of Sir2 enzyme with QM/MM approach: SN1 vs SN2? *The Journal of physical chemistry, B* 114(36):11927-11933.
28. Shi YW, Zhou YZ, Wang SL, & Zhang YK (2013) Sirtuin Deacetylation Mechanism and Catalytic Role of the Dynamic Cofactor Binding Loop. *J. Phys. Chem. Lett.* 4(3):491-495.
29. Avalos JL, Bever KM, & Wolberger C (2005) Mechanism of sirtuin inhibition by nicotinamide: Altering the NAD(+) cosubstrate specificity of a Sir2 enzyme. *Molecular Cell* 17(6):855-868.
30. Guan X, Lin P, Knoll E, & Chakrabarti R (2014) Mechanism of inhibition of the human sirtuin enzyme SIRT3 by nicotinamide: computational and experimental studies. *PLoS One* 9(9):e107729.
31. Cen Y & Sauve AA (2010) Transition state of ADP-ribosylation of acetyllysine catalyzed by *Archaeoglobus fulgidus* Sir2 determined by kinetic isotope effects and computational approaches. *Journal of the American Chemical Society* 132(35):12286-12298.
32. Sauve AA, Moir RD, Schramm VL, & Willis IM (2005) Chemical activation of Sir2-dependent silencing by relief of nicotinamide inhibition. *Molecular Cell* 17(4):595-601.
33. Hawse WF, et al. (2008) Structural Insights Into Intermediate Steps in the Sir2 Deacetylation Reaction. *Structure* 16(9):1368-1377.
34. Jin L, et al. (2009) Crystal Structures of Human SIRT3 Displaying Substrate-induced Conformational Changes. *The Journal of Biological Chemistry*. 284(36): 24394-24405.
35. Armstrong CM, Kaeberlein M, Imai SI, & Guarente L (2002) Mutations in *Saccharomyces cerevisiae* gene SIR2 can have differential effects on in vivo silencing phenotypes and in vitro histone deacetylation activity. *Mol Biol Cell* 13(4):1427-1438.
36. Szczepankiewicz BG, et al. (2012) Synthesis of carba-NAD and the structures of its ternary complexes with SIRT3 and SIRT5. *The Journal of organic chemistry* 77(17):7319-7329.
37. Zhao KH, Harshaw R, Chai XM, & Marmorstein R (2004) Structural basis for nicotinamide cleavage and ADP-ribose transfer by NAD(+) -dependent Sir2 histone/protein deacetylases. *Proceedings of the National Academy of Sciences of the United States of America* 101(23):8563-8568.
38. Sauve AA & Schramm VL (2003) Sir2 regulation by nicotinamide results from switching between base exchange and deacetylation chemistry. *Biochemistry* 42(31):9249-9256.
39. Hockerman GH, Peterson BZ, Johnson BD, & Catterall WA (1997) Molecular determinants of drug binding and action on L-type calcium channels. *Annual review of pharmacology and toxicology* 37:361-396.
40. Mai A, et al. (2009) Study of 1,4-dihydropyridine structural scaffold: discovery of novel sirtuin activators and inhibitors. *J Med Chem* 52(17):5496-5504.
41. Jackson MD, Schmidt MT, Oppenheimer NJ, & Denu JM (2003) Mechanism of nicotinamide inhibition and transglycosylation by Sir2 histone/protein deacetylases. *The Journal of biological chemistry* 278(51):50985-50998.
42. Sauve AA & Schramm VL (2003) Nicotinamide inhibition of SIR2 is a consequence of chemical competition for an ADPR - peptidyl intermediate. *Biochemistry* 42(28):8630-8630.
43. Imai S (2010) A possibility of nutraceuticals as an anti-aging intervention: Activation of sirtuins by promoting mammalian NAD biosynthesis. *Pharmacological research : the official journal of the Italian Pharmacological Society* 62(1):42-47.
44. Pacholec M, et al. (2010) SRT1720, SRT2183, SRT1460, and Resveratrol Are Not Direct Activators of SIRT1. *Journal of Biological Chemistry* 285(11):8340-8351.
45. Wang G, et al. (2014) P7C3 neuroprotective chemicals function by activating the rate-limiting enzyme in NAD salvage. *Cell* 158(6):1324-1334.
46. Hawse WF & Wolberger C (2009) Structure-based Mechanism of ADP-ribosylation by Sirtuins. *Journal of Biological Chemistry* 284(48):33654-33661.
47. Chakrabarti R, Klibanov AM, Friesner RA (2005) Sequence optimization and designability of enzyme active sites. *Proceedings of the National Academy of Sciences of the United States of America* 102: 12035-12040.

1293  
1294  
1295  
1296  
1297  
1298  
1299  
1300  
1301  
1302  
1303  
1304  
1305  
1306  
1307  
1308  
1309  
1310  
1311  
1312  
1313  
1314  
1315  
1316  
1317  
1318  
1319  
1320  
1321  
1322  
1323  
1324  
1325  
1326  
1327  
1328  
1329  
1330  
1331  
1332  
1333  
1334  
1335  
1336  
1337  
1338  
1339  
1340  
1341  
1342  
1343  
1344  
1345  
1346  
1347  
1348  
1349  
1350  
1351  
1352  
1353  
1354  
1355  
1356  
1357  
1358  
1359  
1360

Please review all the figures in this paginated PDF and check if the figure size is appropriate to allow reading of the text in the figure.

If readability needs to be improved then resize the figure again in 'Figure sizing' interface of Article Sizing Tool.